JACS
JOURNAL OF THE AMERICAN CHEMICAL SOCIETY

ARTICLE

pubs.acs.org/JACS

A Generalized Ligand-Exchange Strategy Enabling Sequential Surface Functionalization of Colloidal Nanocrystals

Angang Dong,*[,†,∥] Xingchen Ye,[†] Jun Chen,[‡] Yijin Kang,[†] Thomas Gordon,[†] James M. Kikkawa,[§] and Christopher B. Murray*[,†,‡]

[†]Department of Chemistry, [‡]Department of Materials Science and Engineering, and [§]Department of Physics & Astronomy, University of Pennsylvania, Philadelphia, Pennsylvania 19104, United States

[∥]The Molecular Foundry, Lawrence Berkeley National Laboratory, Berkeley, California 94720, United States

Supporting Information

ABSTRACT: The ability to engineer surface properties of nanocrystals (NCs) is important for various applications, as many of the physical and chemical properties of nanoscale materials are strongly affected by the surface chemistry. Here, we report a facile ligand-exchange approach, which enables sequential surface functionalization and phase transfer of colloidal NCs while preserving the NC size and shape. Nitrosonium tetrafluoroborate ($NOBF_4$) is used to replace the original organic ligands attached to the NC surface, stabilizing the NCs in various polar, hydrophilic media such as *N*,*N*-dimethylformamide for years, with no observed aggregation or precipitation. This approach is applicable to various NCs (metal oxides, metals, semiconductors, and dielectrics) of different sizes and shapes. The hydrophilic NCs obtained can subsequently be further functionalized using a variety of capping molecules, imparting different surface functionalization to NCs depending on the molecules employed. Our work provides a versatile ligand-exchange strategy for NC surface functionalization and represents an important step toward controllably engineering the surface properties of NCs.

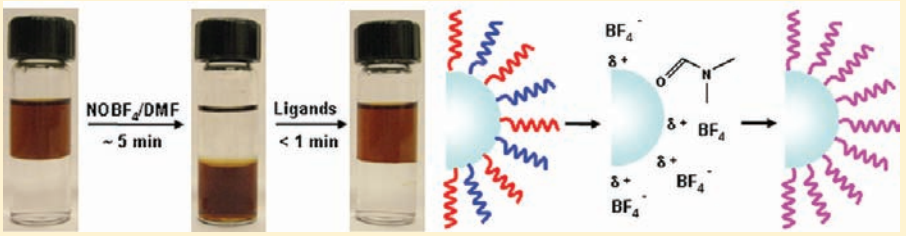

1. INTRODUCTION

Inorganic nanocrystals (NCs) are useful in many areas including electronics,[1−3] optoelectronics,[4−6] catalysis,[7−9] magnetics,[10−13] and biotechnology,[14−16] due to their unique size- and shape-dependent properties. Because of recent advances in colloidal chemistry, the inventory of monodisperse NCs has been expanded from metals[17,18] and semiconductors[19−21] to magnetic[10,22,23] and dielectric[16,24] materials. Most synthetic routes to high-quality NCs with tunable sizes and shapes predominantly employ long hydrocarbon molecules containing a coordinating headgroup such as oleic acid (OA) and oleylamine (OAm) as ligands,[25] which sterically stabilize NCs in nonpolar, hydrophobic solvents as well as play a key role in the self-assembly of ordered NC arrays or superlattices.[26] However, the presence of such bulky capping molecules creates an insulating barrier around each NC and blocks the access of molecular species to the NC surface, which is detrimental for electronic[2,27] and catalytic[28] applications. In addition, biological applications generally require NCs to be fully dispersible in hydrophilic or aqueous media without property degradation.[29−31] To address these problems, the as-synthesized NCs must undergo surface treatment or modification, typically by replacing the original ligands with specifically designed species through a ligand-exchange process.[32] To transfer NCs into aqueous media, a number of nonexchange approaches have also been developed by using amphiphilic molecules to coordinate with the surface ligands through hydrophobic van der Waals interactions.[33−36] Although surface modification based on ligand-exchange reactions has been actively explored in various NC systems,[37−45] a generalized and efficient strategy is far from developed. In addition, excluding a few surface modification approaches that allow reversible phase transfer of NCs,[40,41] most ligand-exchange reactions utilize stronger surface-binding molecules to displace the original ligands, such that the exchange process is typically irreversible,[2] making it difficult to further functionalize NCs.

Recently, Talapin and co-workers introduced a new surface-modification approach using highly nucleophilic metal chalcogenide complexes (MCCs), such as $Sn_2S_6^{4-}$ and $In_2Se_4^{2-}$, for ligand exchange, allowing phase transfer of NCs from a hydrophobic solvent to various hydrophilic media.[43,44] The reduced interparticle spacing that results from the exchange of long hydrocarbon molecules with the much smaller MCC clusters enables strong electronic coupling between neighboring NCs, yielding highly conductive NC films. This surface modification strategy proves to be applicable to semiconductor (e.g., CdSe and

Received: October 4, 2010
Published: December 22, 2010

Bi_2S_3, etc.) and metal (e.g., Au) NCs;[43] however, extensions of this approach to other materials such as metal oxides and dielectrics have not yet been reported. In addition, MCCs are typically synthesized in the highly toxic and pyrophoric hydrazine medium, such that the ligand-exchange reactions must be performed with great caution under inert environment,[43−45] which limits the wide application of the approach.

In this work, we report a more generalized ligand-exchange strategy, which enables sequential surface modification and phase transfer of NCs without affecting the NC size and shape. Nitrosonium tetrafluoroborate ($NOBF_4$) or diazonium tetrafluoroborate compounds are employed to replace the original ligands, thus stabilizing the NCs in various polar, hydrophilic media such as *N*,*N*-dimethylformamide (DMF), dimethylsulfoxide (DMSO), or acetonitrile. Fourier-transform infrared (FTIR) spectroscopy, ζ-potential measurements, and thermogravimetric analysis (TGA) establish the replacement of organic ligands by inorganic BF_4^- anions, which provide electrostatic stabilization of the NCs in the polar media. The generality of the approach is demonstrated for various NCs having different compositions, sizes, and shapes. In comparison with previous surface modification strategies, one distinct advantage of the present approach is that the hydrophilic NCs obtained, regardless of the NC composition and morphology, can be readily further functionalized by various capping molecules via a secondary ligand-exchange reaction, allowing fully reversible phase transfer and surface functionalization of NCs. This provides a vast opportunity to engineer surface properties of NCs by introducing functional capping molecules.

2. EXPERIMENTAL SECTION

Chemicals. The following chemicals were purchased and used as received. $NOBF_4$ (97%), 4-bromobenzenediazonium tetrafluoroborate (96%), NH_4BF_4, tetramethylammonium tetrafluoroborate, hexylamine (HAm, 99%), DMSO, DMF, acetonitrile, and dichloromethane were obtained from Acros. OA (90%), OAm (70%), 4-nitrobenzenediazonium tetrafluoroborate (97%), and poly(vinyl pyrollidone) (PVP, average MW ∼55 000) were purchased from Aldrich. Tetradecylphosphonic acid (TDPA, 97%) was obtained from Alfa Aesar.

Synthesis and Purification of Colloidal NCs. All preparative procedures were conducted using standard Schlenk-line techniques in dry glassware under a dry N_2 atmosphere. Monodisperse Fe_3O_4,[22] FePt,[10] and $CoPt_3$[23] NCs, TiO_2 nanorods (∼3 nm × 20 nm),[46] Bi_2S_3 nanorods (∼8 nm × 80 nm),[47] and rare-earth doped upconversion $NaYF_4$ nanorods (∼30 nm × 50 nm) and hexagonal nanoplates (∼200 nm × 100 nm)[24] stabilized by OA and/or OAm were synthesized according to literature methods. The as-synthesized NCs were purified by precipitation with the addition of ethanol, and the precipitated NCs were redispersed in hexane to form stable colloidal dispersions with concentrations of 1−10 mg/mL.

Ligand-Exchange Reactions of Colloidal NCs. In a typical process, 5 mL of NC dispersion in hexane (∼5 mg/mL) was combined with 5 mL of dichloromethane solution of $NOBF_4$ (0.01 M) at room temperature. The resulting mixture was shaken gently until the precipitation of NCs was observed, typically within 5 min. After centrifugation to remove the supernatant, the precipitated NCs can be redispersed in various hydrophilic media such as DMF, DMSO, or acetonitrile. To purify NCs, toluene and hexane (1:1 by volume) were added to flocculate the NC dispersion. After centrifugation, the aforementioned polar solvent was added to redisperse NCs to form a stable colloidal dispersion. This ligand-exchange reaction can also be carried out based on a phase transfer process. In this procedure, the NC hexane dispersion was first combined with acetonitrile to form a two-phase mixture, into which an appropriate amount of $NOBF_4$ was added. The resulting mixture was stirred until NCs were transferred from the upper hexane layer to the bottom acetonitrile layer, typically within 5 min. The surface-modified NCs were then purified by precipitation with the addition of toluene, and the precipitated NCs were redispersed in various hydrophilic media.

The ligand-exchange reactions with diazonium tetrafluoroborate compounds such as 4-nitrobenzenediazonium tetrafluoroborate or 4-bromobenzenediazonium tetrafluoroborate were conducted as follows. The NC hexane dispersion was combined with DMF to form a two-phase mixture, into which an appropriate amount of 4-nitrobenzenediazonium (or 4-bromobenzenediazonium) tetrafluoroborate was added. The resulting mixture was vigorously stirred until NCs were transferred from the upper hexane layer to the bottom DMF layer, typically within 30 min. NCs were purified following the same procedure as described above.

Secondary Ligand-Exchange Reactions of NCs. The hydrophilic NCs obtained by $NOBF_4$ or diazonium tetrafluoroborate treatments can be further functionalized by various capping molecules such as OA, OAm, TDPA, or HAm through a secondary ligand-exchange reaction, enabling fully reversible phase transfer of NCs between hydrophobic and hydrophilic media. In a typical process, 5 mL of hexane was first combined with a DMF dispersion of the hydrophilic NCs (5 mL, ∼5 mg/mL) to form a two-phase mixture, into which an appropriate amount of the aforementioned capping molecules was added. A subsequent brief shaking (∼1 min) led to the phase transfer of NCs from the DMF layer to the hexane layer, indicating the successful binding of organic ligands to the NC surface. The NCs were precipitated by addition of ethanol. After centrifugation to remove the supernatant, the precipitated NCs were redispersed in hexane to form a stable colloidal dispersion. When HAm was used as the capping molecules, toluene instead of hexane was used to redisperse NCs. To transfer NCs to an aqueous medium, PVP was used for the secondary ligand-exchange reaction. Briefly, 50 mg of PVP was added into a DMF dispersion of the hydrophilic NCs (5 mL, ∼5 mg/mL) followed by vigorous stirring (30 min). The NCs were precipitated by addition of acetone, and the precipitated NCs were redispersed in water to form a stable dispersion.

Characterization. Transmission electron microscopy (TEM) images were recorded using a JEOL-1400 TEM equipped with a SC1000 ORIUS CCD camera operating at 120 kV. The sample was prepared by drop-casting a NP dispersion on a carbon-coated TEM grid followed by drying in air. Magnetization measurements of Fe_3O_4 NCs were performed on a superconducting quantum interference device (SQUID) from Quantum Design. FTIR spectra were acquired in the transmission mode using a Nicolet 8700 FTIR spectrometer. The samples were prepared by drop-casting concentrated NC dispersions on KBr substrates (International Crystal Laboratories) followed by drying in air to form a thin NC film. To quantitatively compare FTIR spectra before and after ligand exchange, the absorbance was normalized to the weight of the absorbing materials deposited per unit area of the substrate, and the spectra were baseline-corrected.[43] Dynamic light scattering (DLS) and ζ-potential data were collected on a Beckman Coulter Delsa Nano-C system. TGA was conducted using a TA Instruments SDT Q600 at a heating rate of 5 °C/min under N_2. Upconversion luminescence spectra of rare-earth doped $NaYF_4$:Yb/Er and $NaYF_4$:Yb/Tm NCs were recorded on a USB4000 fluorescence spectrometer (Ocean Optics) under 980 nm excitation using a diode laser (power density of ∼50 mW/cm^2). Electrochemical measurements of FePt and $CoPt_3$ NCs were performed on a potentiostat (Epsilon, Bioanalytical Systems Inc.) equipped with a rotating disk electrode (RDE). The working electrode was prepared by drop-casting a concentrated NC dispersion onto the RDE followed by drying in air. The Ag/AgCl electrode was used as the reference electrode, with a platinum coil as the counter electrode and $HClO_4$ (0.1 M) as the electrolyte. The

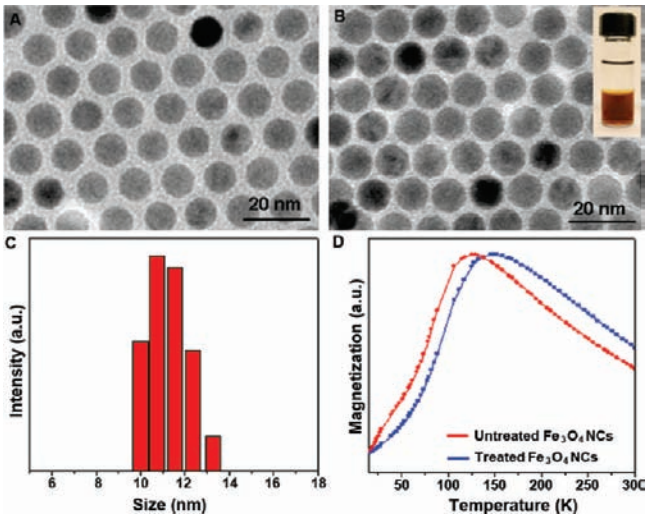

Figure 1. TEM images of Fe_3O_4 NCs (A) before and (B) after $NOBF_4$ treatment. The inset in (B) shows the photograph of the BF_4^--modified Fe_3O_4 NCs dispersed in DMF, with the upper layer of hexane. (C) DLS measurement of the BF_4^--modified Fe_3O_4 NCs dispersed in DMF, showing the aggregate-free nature of the colloidal dispersion. (D) Zero-field-cool magnetizations of Fe_3O_4 NCs before and after $NOBF_4$ treatment, respectively, showing an increase of the blocking temperature upon surface modification.

cyclic voltammetry measurements were carried out at room temperature under a flow of nitrogen gas at a sweep rate of 100 mV/s. Formic acid oxidation reactions were carried out in a solution of 0.1 M $HClO_4$ and 0.5 M formic acid at a sweep rate of 20 mV/s, with the second sweeps recorded.

3. RESULTS AND DISCUSSION

Surface Modification of NCs by $NOBF_4$ Treatment. The as-synthesized NCs are soluble in nonpolar, hydrophobic solvents such as hexane due to the presence of organic ligands (i.e., OA and/or OAm) on the NC surface. When the dichloromethane solution of $NOBF_4$ is added to the NC dispersion in hexane, NCs are found to precipitate immediately after gentle shaking, indicating a dramatic change in NC solubility as a result of surface modification. After centrifugation to remove the supernatant, the precipitated NCs can be readily redispersed in various polar, hydrophilic solvents such as DMF, DMSO, or acetonitrile to form colloidal dispersions. In particular, NCs dispersions in DMF are stable for several years without any detectable aggregation or precipitation. Attempts to directly redisperse NCs in water result in partial aggregation, while the addition of a small amount of DMF in water (~1:20 by volume) yields stable colloidal dispersions.

Figure 1 shows TEM images of 10 nm Fe_3O_4 NCs before and after $NOBF_4$ treatment, respectively, revealing that the NC size and shape are preserved and no NC aggregation is observed upon surface modification (Figure 1A and B). The aggregate-free nature of the NC dispersions in DMF is further verified by the monomodal size distributions measured by DLS (Figure 1C). TEM also shows that the average interparticle spacing is reduced from 3.0 to 1.2 nm upon $NOBF_4$ treatment, indicative of the removal of the long hydrocarbon ligands. This reduced interparticle distance enhances magnetic dipolar coupling interactions between neighboring Fe_3O_4 NCs, and as a result the blocking temperature (T_B) increases from ~127 to ~147 K

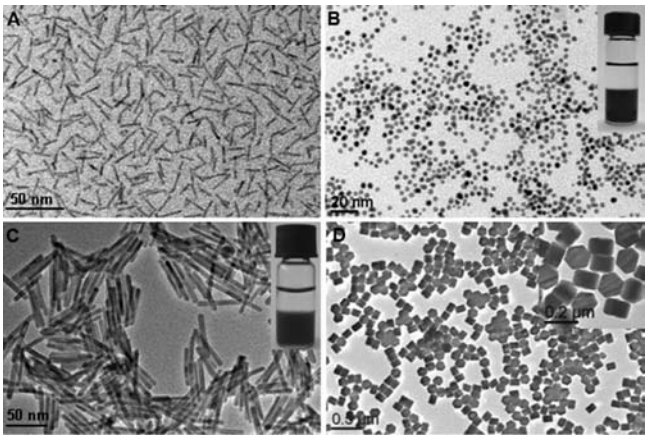

Figure 2. TEM images of the BF_4^--modified NCs dispersed in DMF: (A) TiO_2 nanorods (~3 nm × 20 nm), (B) FePt NCs (4 nm), (C) Bi_2S_3 nanorods (~8 nm × 80 nm), and (D) upconversion $NaYF_4$ nanoplates (~200 nm × 100 nm). The insets in (B) and (C) show photographs of the BF_4^--modified NCs dispersed in DMF, with the upper layer of hexane. The inset in (D) shows a high-magnification TEM image.

(Figure 1D). The influence of dipolar interactions on T_B has been a matter of some controversy, with many suggesting an increase with stronger interactions,[48−51] while others claim exactly the opposite.[52] The systems discussed here are well suited to test the effects of interactions because exchange interactions can be assumed negligible and are consistent with an increase in T_B with increasing dipolar interactions.

Significantly, this surface modification strategy is applicable to NCs having a variety of compositions, sizes, and shapes, including metal oxides such as Fe_3O_4 (10 nm, Figure 1) and TiO_2 nanorods (~3 nm × 20 nm, Figure 2A), metal alloys such as FePt (4 nm, Figure 2B) and $CoPt_3$ NCs, semiconductors such as Bi_2S_3 nanorods (~8 nm × 80 nm, Figure 2C), and dielectrics such as rare-earth doped upconversion $NaYF_4$ nanorods (~30 nm × 50 nm) and nanoplates (~200 nm × 100 nm, Figure 2D). It should be mentioned that our attempts to apply this approach to other semiconductor quantum dots such as PbS and PbTe result in unstable colloidal DMF dispersions with significant NC agglomeration or fusion (Figure S1).

The hydrophilic nature and the reduced interparticle spacing of the surface-modified NCs suggest the removal of the original organic ligands, which is further confirmed by FTIR spectroscopy. The FTIR spectra of Fe_3O_4 NCs in Figure 3A show that the intensity of the characteristic C−H stretching vibrations at 2800−3000 cm^{-1} ascribed to OA molecules is noticeably reduced after surface treatment. The quantitative comparison shows $NOBF_4$ treatment removes 80−85% of the original OA molecules attached to the NC surface. We further investigate the species stripped from the NC surface during the ligand-exchange process, which are retrieved by drying the supernatant solution (i.e., hexane and dichloromethane) after the collection of NCs. The FTIR spectrum of the dried residues is very similar to that of OA (Figure S2), confirming that OA capping molecules are indeed displaced from the NC surface during $NOBF_4$ treatment. The broad band around 3500 cm^{-1} is assigned to the solvated water molecules, consistent with the hydrophilic nature of the NC dispersion. In comparison with the FTIR spectrum of the untreated NCs, a new peak at 1084 cm^{-1} emerges after ligand exchange, which is assigned to BF_4^- anions,[53] while no bands ascribed to NO^+ (~2100−2200 cm^{-1})[54] are detectable in the

dx.doi.org/10.1021/ja108948z |J. Am. Chem. Soc. 2011, 133, 998–1006

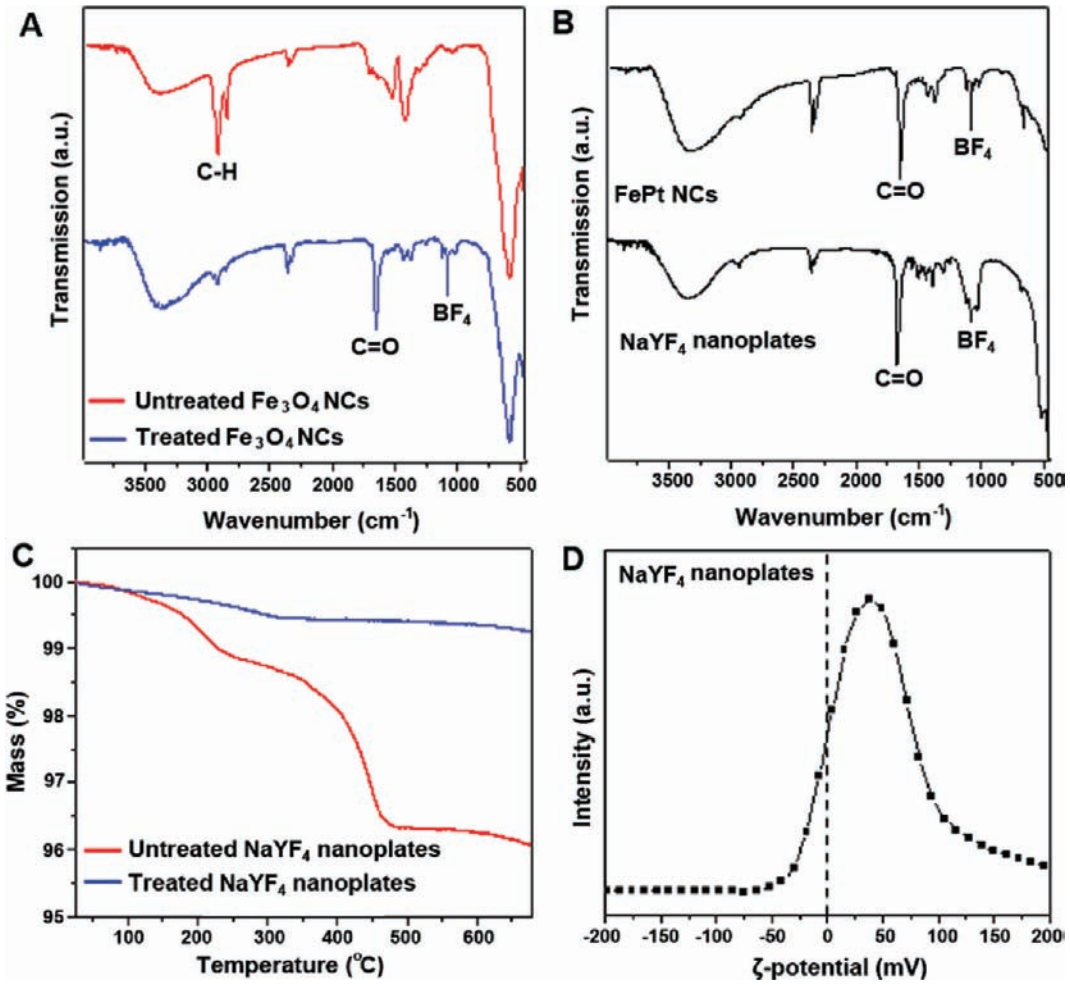

Figure 3. (A) FTIR spectra of Fe_3O_4 NCs before and after $NOBF_4$ treatment, respectively. (B) FTIR spectra of the BF_4^--modified FePt NCs and upconversion $NaYF_4$ nanoplates, respectively. (C) TGA scans of upconversion $NaYF_4$ nanoplates before and after $NOBF_4$ treatment, respectively. (D) ζ-Potential measured for the BF_4^--modified upconversion $NaYF_4$ nanoplates dispersed in DMF.

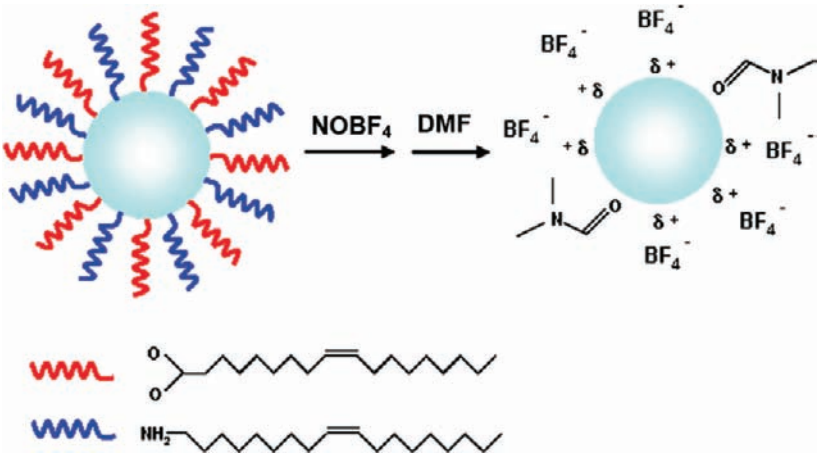

Figure 4. Schematic illustration of the ligand-exchange process with $NOBF_4$.

FTIR spectrum (Figure 3A). These results suggest an exchange between the organic ligands and inorganic BF_4^- anions. The remaining new peak around 1650 cm^{-1} can be attributed to C═O stretching vibrations of the solvent DMF molecules, as no peaks in this region are observed when the surface-modified NCs are redispersed in acetonitrile or DMSO. The presence of DMF at the NC surface indicates that DMF molecules act as costabilizers to protect NCs from aggregation. This also explains the exceptionally high solubility and stability of the NC dispersions in DMF. Notably, very similar FTIR spectra are acquired for

dx.doi.org/10.1021/ja108948z |J. Am. Chem. Soc. 2011, 133, 998–1006

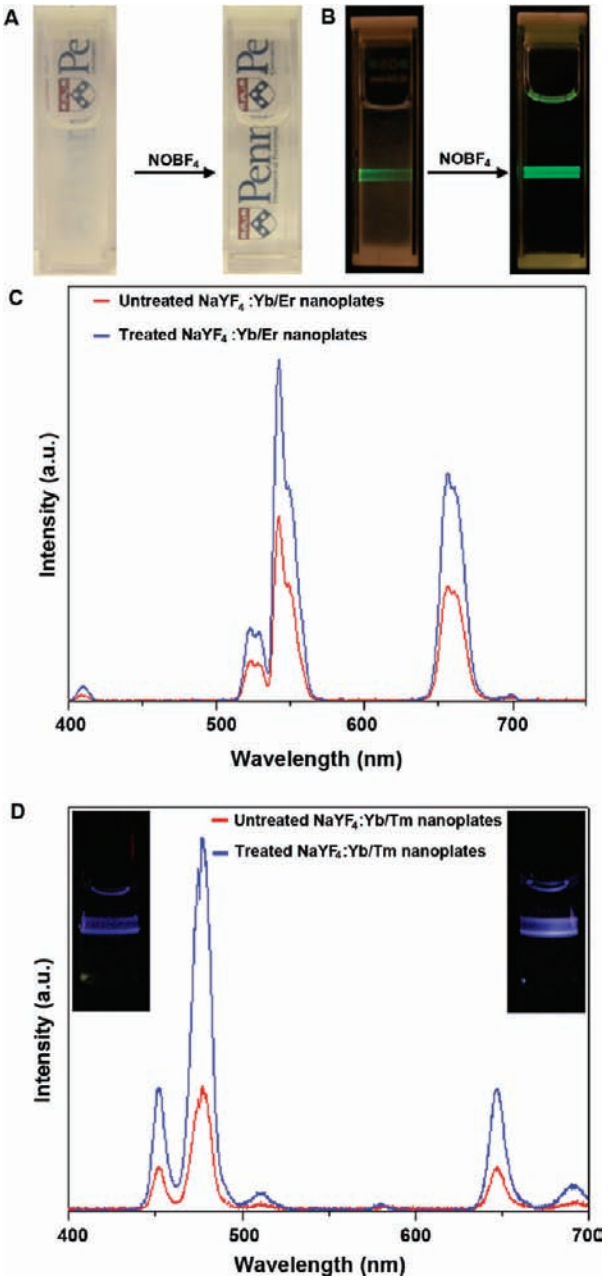

Figure 5. Enhanced colloidal solubility and emission intensity of upconversion $NaYF_4$ nanoplates. Photographs of (A) colloidal dispersions and (B) visible upconversion luminescence of $NaYF_4$:Yb/Er nanoplates before and after $NOBF_4$ treatment, respectively. The NC concentrations are kept the same before and after surface modification. (C) Comparison of the upconversion emission spectra of $NaYF_4$:Yb/Er nanoplates before and after $NOBF_4$ treatment. (D) Comparison of upconversion emission spectra of $NaYF_4$:Yb/Tm nanoplates before and after $NOBF_4$ treatment, with the corresponding visible upconversion luminescence shown in the upper left and upper right insets, respectively.

other surface-modified NCs such as FePt and $NaYF_4$ (Figure 3B), leading us to conclude that this exchange mechanism is universal for a variety of NCs having different sizes and shapes.

Figure 3C shows the TGA studies of $NaYF_4$ nanoplates before and after $NOBF_4$ treatment, respectively, which are collected by heating the sample from room temperature to 650 °C under N_2. The total weight loss of the surface-modified NCs is only 0.5%,

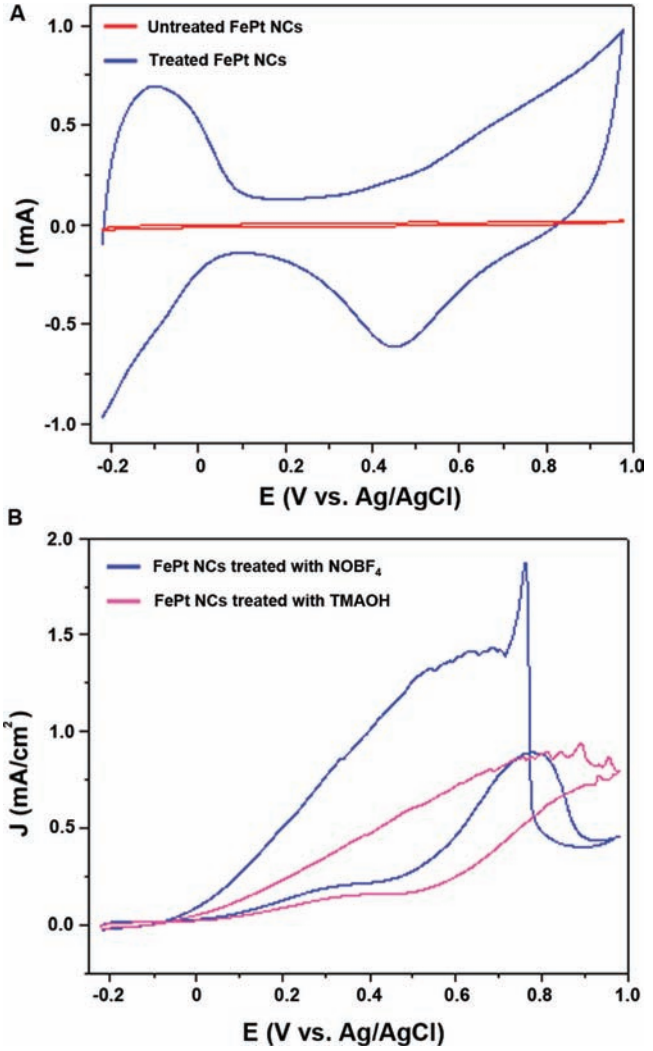

Figure 6. (A) Cyclic voltammograms of $Fe_{0.5}Pt_{0.5}$ NCs (4 nm) before and after $NOBF_4$ treatment, respectively, showing the enhanced active Pt surface area after surface modification. (B) Formic acid oxidation polarization curves for $Fe_{0.5}Pt_{0.5}$ NCs treated with $NOBF_4$ and TMAOH, respectively.

much lower than that of the untreated sample (~4%), providing further evidence for the nearly complete exchange of organic ligands by inorganic BF_4^- anions. Electrophoretic mobility and ζ-potential measurements show that after surface modification, NCs dispersed in DMF are positively charged regardless of the NC compositions (Figures 3D and S3). Because FTIR spectroscopy confirms the absence of NO^+ cations, we attribute the positive charges to the uncoordinated metal cations arising from the removal of organic ligands at the NC surface. It is interesting to note that BF_4^- itself does not have a strong binding affinity to the NC surface, as phase transfer and surface modification of NCs cannot be achieved in control experiments when $NOBF_4$ is replaced by NH_4BF_4 or tetramethylammonium tetrafluoroborate. Unlike NH_4^+ or tetramethylammonium cations, NO^+ is a good leaving group as it is readily reduced to NO, which is then oxidized to NO_2 by oxygen during the ligand-exchange process. On the other hand, NO^+ reacts readily with the solvated water molecules to form nitrous acid (pK_a=3.4) and fluoroboric acid (pK_a = −0.4), producing a fairly acidic environment. Even after purification, the NC dispersion in DMF is acidic with a pH value

dx.doi.org/10.1021/ja108948z |J. Am. Chem. Soc. 2011, 133, 998–1006

of ~3−5. As a result, the rapid removal of NO^+ cations results in a considerable amount of BF_4^- anions and protons remaining in the NC dispersion. We hypothesize that the acidic protons will facilitate the removal of the original organic ligands by protonation,[40] thus promoting the coordination of the BF_4^- anions with the positively charged surface metal centers (metal cations or oxidized metal atoms), as schematically illustrated in Figure 4. The removal of organic ligands and the subsequent coordination of BF_4^- anions and DMF to the NC surface impart hydrophilicity to NCs. This hypothesis is also supported by the fact that similar surface modification of NCs by BF_4^- anions can also be achieved by using diazonium tetrafluoroborate compounds such as 4-nitrobenzenediazonium tetrafluoroborate or 4-bromobenzenediazonium tetrafluoroborate. As in the case of $NOBF_4$ treatment, FTIR spectroscopy shows no evidence of diazonium cations and confirms the presence of BF_4^- anions and DMF after exchange (Figure S4), implying that the substitution reaction is likely to be driven by the removal of diazonium cations.

Colloidal Solubility and Stability of the BF_4^--Modified NCs. As mentioned above, the BF_4^--modified NCs are highly soluble in DMF due to the dual stabilization from BF_4^- and DMF. The NC solubility is even higher than the initial solubility in hexane, especially for large sized NCs. For example, colloidal dispersions of OA-capped upconversion $NaYF_4$:Yb/Er nanoplates (~200 nm × 100 nm) are unstable in hexane due to their large size and thus precipitate from the dispersion very quickly (typically within 10 min). The cloudy appearance of the colloidal dispersion originating from the strong light scattering demonstrates the limited NC solubility in hexane (Figure 5A). In contrast, the solubility is significantly improved when $NaYF_4$ nanoplates are dispersed in DMF after $NOBF_4$ treatment, as evidenced by the transparency (Figure 5A) as well as the high stability of the colloidal dispersion. Even highly concentrated colloidal dispersions (~5 mg/mL) are stable for several months without sedimentation or precipitation despite the large NC size. Notably, this improved NC solubility leads to an enhancement in upconversion emission intensity, as seen in Figure 5B. We speculate that the improved NC solubility reduces the scattering of the incident laser light, which increases the excitation efficiency and therefore effectively enhances the emission intensity.

To quantify the emission enhancement, we measure the photoluminescence spectra of these upconversion NCs by exciting the colloidal dispersions with a 980 nm diode laser, with NC concentrations kept constant before and after surface modification. As compared to the untreated $NaYF_4$:Yb/Er nanoplates dispersed in hexane, a significant increase in emission intensity (enhancement factor: ~2) is observed when the BF_4^--modified nanoplates are dispersed in DMF (Figure 5C). Similarly, this enhanced emission intensity is also observed for the upconversion $NaYF_4$:Yb/Tm nanoplates (enhancement factor: ~3) (Figure 5D), indicating that the enhancement is independent of the emission wavelength. It should be mentioned that when smaller upconversion $NaYF_4$:Yb/Er nanorods (~30 nm × 50 nm), which can form transparent and stable dispersions in hexane, are subjected to a similar $NOBF_4$ treatment, the emission intensity remains virtually unchanged (Figure S5), implying that the observed emission enhancement for the upconversion $NaYF_4$ nanoplates indeed results from the improved NC solubility rather than surface capping or solvent effect.

Electrocatalytic Properties of the BF_4^--Modified Pt-Based Alloyed NCs. NCs of Pt-based alloys such as FePt and $CoPt_3$ are promising electrocatalysts for fuel cell applications.[55−58] Recent efforts to improve the performance of Pt-based catalysts have been focused on the optimization of particle size, shape, and composition.[28] To enable catalytic applications, the original organic ligands attached to the NC surface need to be removed, generally by UV/ozone[28,55] or thermal annealing treatment.[57,58] However, UV/ozone treatment only works efficiently for very thin films and is limited to materials that can survive the strong oxidative environment. Thermal annealing, on the other hand, can result in sintering or agglomeration of metallic NCs, which will inevitably reduce the catalytic performance. It is therefore desirable to design new surface treatment strategies that allow the removal of organic ligands while preserving the particle's morphology and solution processability. $NOBF_4$ treatment described here appears to meet all these requirements. Figure 6A shows the cyclic voltammetry measurements of $Fe_{0.5}Pt_{0.5}$ NCs (4 nm) before and after $NOBF_4$ treatment, respectively. As expected, the nearly featureless voltammogram of the untreated NCs indicates that the NC surface is completely capped by long hydrocarbon molecules, blocking the access of hydrogen molecules to the surface Pt atoms, whereas a dramatic enhancement of the active Pt surface area is observed after $NOBF_4$ treatment (Figure 6A). The voltammetric feature of the BF_4^--modified NCs is very similar to that of the sample subjected to UV/ozone treatment,[55] indicative of the potential for electrocatalytic applications. In addition to FePt NCs, $CoPt_3$ NCs show similar enhancement in the active Pt surface area upon $NOBF_4$ treatment, demonstrating the generality of this approach. We surmise that BF_4^- anions are likely coordinating with the surface Fe (or Co) cations that are formed by oxidation, such that the uncoordinated surface Pt atoms are exposed for hydrogen access, leading to the significant enhancement in the active Pt surface area.

To evaluate the catalytic activity, we test the electrocatalytic properties of the BF_4^--modified FePt NCs for formic acid

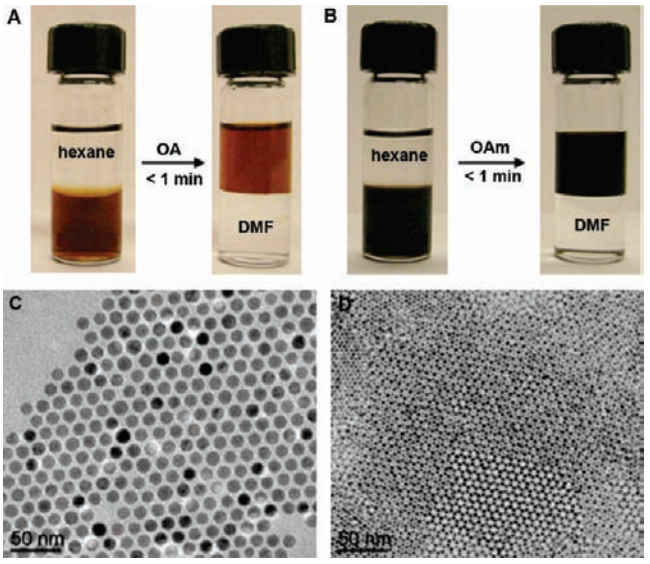

Figure 7. Surface functionalization of the BF_4^--modified NCs by a secondary ligand-exchange process. Photographs of colloidal dispersions of (A) Fe_3O_4 and (B) FePt NCs, showing that the BF_4^--modified NCs initially dispersed in the bottom DMF layer are transferred to the upper hexane layer upon the addition of organic ligands. TEM images of (C) OA-capped Fe_3O_4 and (D) OAm-capped FePt NCs after the secondary ligand-exchange process, showing the self-assembled superlattice structure.

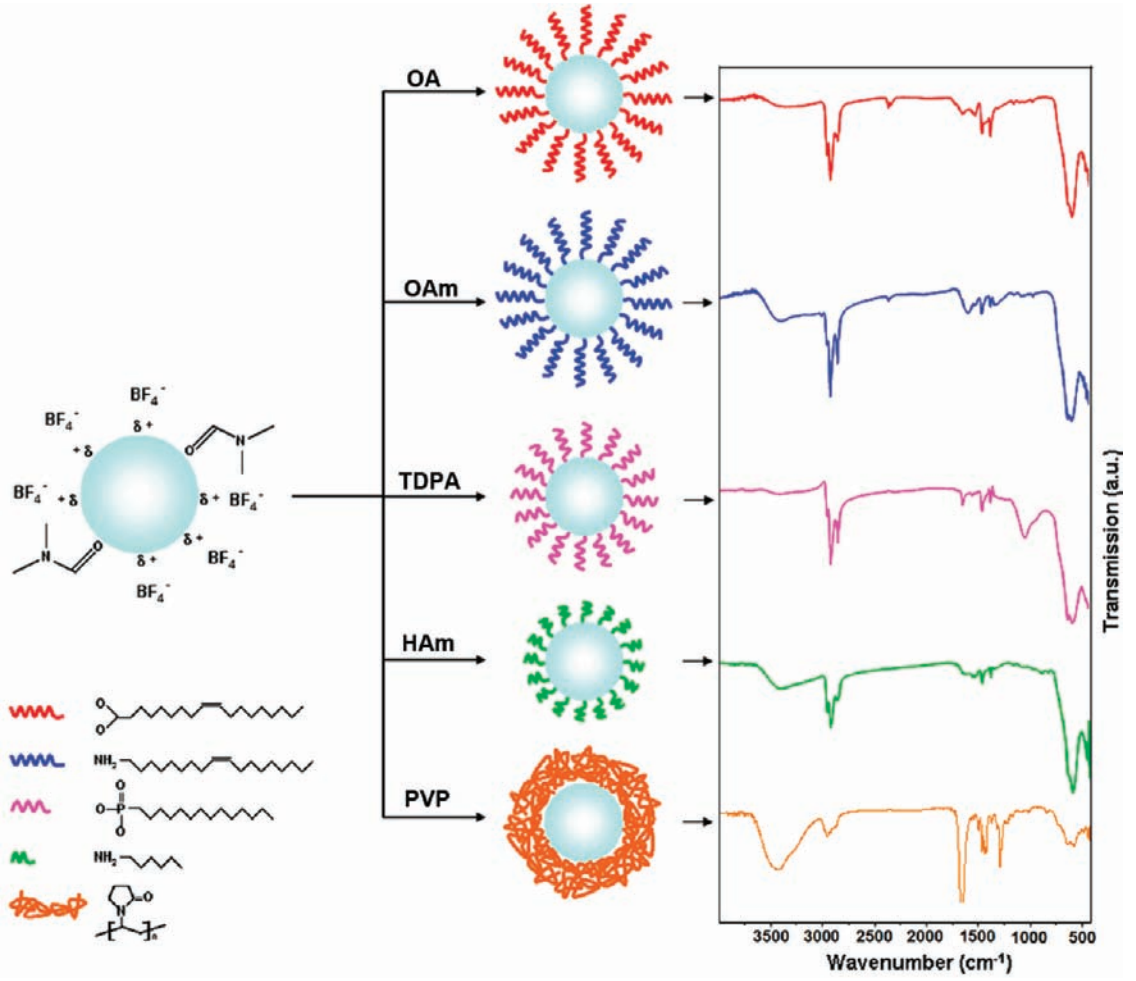

Figure 8. Schematic illustration of the secondary ligand-exchange process, showing the surface functionalization of the BF_4^--modified Fe_3O_4 NCs by various capping molecules. The right column shows the corresponding FTIR spectra.

oxidation reactions. The catalytic performance is further as compared to the same FePt NCs subjected to tetramethylammounium hydroxide (TMAOH) treatment. TMAOH has been widely used to modify the surface properties of FePt NCs by replacing the organic ligands, enabling phase transfer of NCs to aqueous media.[38] Previous studies have shown that after TMAOH treatment, the NC surface is capped by a layer of hydroxide anions, which in turn is surrounded by a layer of tetramethylammounium counter cations.[38] The polarization curves representing the oxidation activities of the surface-modified FePt NCs are normalized to surface areas, which are calculated by measuring the charge of hydrogen adsorption−desorption. Although the TMAOH-treated FePt NCs exhibit an active Pt surface area similar to that of the $NOBF_4$-treated NCs (Figure S6), their catalytic activity for formic acid oxidation is much lower (Figure 6B), suggesting great potential for the present surface modification approach in catalysis applications.

Secondary Surface Modification of NCs. One of the major benefits of $NOBF_4$ treatment is that the hydrophilic, BF_4^--modified NCs obtained can be further functionalized by a variety of capping molecules regardless of the NC composition and morphology. This allows for fully reversible phase transfer and surface functionalization of NCs. Upon the addition of organic ligands such as OA, OAm, TDPA, or HAm to the NC dispersion in DMF combined with hexane, NCs are found to transfer immediately (<1 min) from the DMF layer to the hexane layer, suggesting that NCs are successfully capped by organic ligands (Figure 7A and B). TEM reveals the preserved NC size and shape after the secondary surface modification, and the formation of ordered NC superlattices provides further evidence of the complete recovery of surface functionalization by organic ligands (Figure 7C and D). The significantly increased C−H stretching intensity and the disappearance of BF_4^- and DMF characteristic peaks in the FTIR spectra also confirm the occurrence of the secondary ligand-exchange reaction (Figures 8 and S7). We attribute this facile reversed surface modification to the weak binding affinity of BF_4^- anions to the NC surface. In addition to hydrophobic capping molecules, the BF_4^--modified NCs can also be functionalized by water-soluble polymers such as PVP, stabilizing NCs in aqueous media without aggregation or precipitation for several months (Figure S8). The stability of the colloidal dispersions is further confirmed by DLS, which reveals the aggregate-free nature of the NC dispersions (Figure S8B). FTIR spectroscopy confirms the presence of PVP at the NC surface after the secondary ligand-exchange reaction (Figure 8). It is noteworthy that no phase transfer is observed in a control experiment when the original Fe_3O_4 NC dispersion in hexane is directly combined with a PVP water solution even after 12 h of vigorous stirring, justifying the necessity of $NOBF_4$ treatment for NC surface functionalization. These results demonstrate that

dx.doi.org/10.1021/ja108948z |*J. Am. Chem. Soc.* 2011, 133, 998–1006

$NOBF_4$ treatment can serve as an intermediate step toward the systematic surface property engineering of NCs by introducing delicately designed functional capping molecules.

4. CONCLUSIONS

We have demonstrated a facile and versatile ligand-exchange strategy to modify the surface properties of NCs by $NOBF_4$ treatment. The replacement of the original organic ligands by inorganic BF_4^- anions enables NCs to be fully dispersible in various polar, hydrophilic solvents without changing the particle size and shape. This ligand-exchange strategy is general for a wide range of colloidal NCs of different sizes and shapes. Upon surface treatment with $NOBF_4$, the NC solubility in DMF is even higher than the initial NC solubility in nonpolar solvents, especially for large sized NCs. The improved NC solubility leads to a significant enhancement in luminescence emission intensity originating from the increased excitation efficiency, as exemplified by the upconversion $NaYF_4$ nanoplates ($\sim$200 nm $\times$ 100 nm). Furthermore, the removal of the bulky organic ligands effectively exposes the NC surface, increasing the catalytic activity of NCs while preserving the solution processability, as demonstrated by FePt NCs. More significantly, the hydrophilic NCs obtained by $NOBF_4$ treatment can readily undergo secondary surface modification due to the weak binding affinity of BF_4^- anions to the NC surface, allowing fully reversible phase transfer of NCs between hydrophobic and hydrophilic media. Although only fairly simplistic organic ligands are demonstrated for the secondary ligand-exchange reactions in this work, it is anticipated that the BF_4^--modified NCs can act as intermediates for the surface functionalization of NCs by more complex capping molecules with programmed functions. The ability to reliably modify NCs with various molecular species provides an exciting opportunity to probe the effect that surface functionalization has on the properties of NCs and NC assemblies, which is important for designing novel NC-based materials for electronic, magnetic, catalytic, and biomedical applications.

■ ASSOCIATED CONTENT

Supporting Information. Figure S1, TEM images of the $NOBF_4$-treated PbS and PbTe NCs; Figure S2, FTIR spectrum of organic residues remaining in the supernatant; Figure S3, ζ-potential measured for various BF_4^--modified NCs dispersed in DMF; Figure S4, FTIR spectrum of $CoPt_3$ NCs treated with 4-bromobenzenediazonium tetrafluoroborate; Figure S5, upconversion emission spectra of $NaYF_4$:Yb/Er nanorods before and after $NOBF_4$ treatment, respectively; Figure S6, cyclic voltammograms of $Fe_{0.5}Pt_{0.5}$ NCs (4 nm) treated with TMAOH; Figure S7, FTIR spectra of FePt NCs capped with various ligands, which are obtained by the secondary ligand-exchange reaction; Figure S8, TEM images and DLS measurement of H_2O-soluble NCs obtained by functionalizing the BF_4^--modified NCs with PVP. This material is available free of charge via the Internet at http://pubs.acs.org.

■ AUTHOR INFORMATION

Corresponding Author

adong@lbl.gov; cbmurray@sas.upenn.edu

■ ACKNOWLEDGMENT

A.D. and C.B.M. acknowledge primary support from the U.S. Army Research Office (ARO) under award number MURI W911NF-08-1-0364 for his roles as experimental lead. C.B.M. is grateful to Richard Perry for the support of his role as project supervisor. This work was partially performed at the Molecular Foundry, Lawrence Berkeley National Laboratory, and was supported by the Office of Science, Office of Basic Energy Sciences, Scientific User Facilities Division, of the U.S. Department of Energy under Contract No. DE-AC02-05CH11231. X.Y.'s contributions with $NaYF_4$ nanophosphors were supported by the Department of Energy's Division of Basic Energy Sciences under award number DE-SC0002158, while T.G.'s development of TiO_2 nanorods was supported by the Nano/Bio Interface Center through the National Science Foundation NSEC under award number DMR08-32802. J.C., Y.K., and J.M.K.'s studies of surface exchanged magnetic nanoparticles were supported through NSF MRSEC program under award number DMR-0520020. We thank Douglas Yates and Lolita Rotkina for the analytical support of the Penn Regional Nanotechnology Facility.

■ REFERENCES

(1) Klein, D. L.; Roth, R.; Lim, A. K. L.; Alivisatos, A. P.; McEuen, P. L. *Nature* **1997,** *389,* 699–701.
(2) Talapin, D. V.; Murray, C. B. *Science* **2005,** *310,* 86–89.
(3) Urban, J. J.; Talapin, D. V.; Shevchenko, E. V.; Kagan, C. R.; Murray, C. B. *Nat. Mater.* **2007,** *6,* 115–121.
(4) Gur, I.; Fromer, N. A.; Geier, M. L.; Alivisatos, A. P. *Science* **2005,** *310,* 462–465.
(5) Luther, J. M.; Law, M.; Beard, M. C.; Song, Q.; Reese, M. O.; Ellingson, R. C.; Nozik, A. J. *Nano Lett.* **2008,** *8,* 3488–3492.
(6) McDonald, S. A.; Konstantatos, G.; Zhang, S.; Cyr, P. W.; Klem, E. J. D.; Levina, L.; Sargent, E. H. *Nat. Mater.* **2005,** *4,* 138–142.
(7) Joo, S. H.; Park, J. Y.; Tsung, C.; Yamada, Y.; Yang, P.; Somorjai, G. A. *Nat. Mater.* **2009,** *8,* 126–131.
(8) Lim, B.; Jiang, M.; Camargo, P. H. C.; Cho, E. C.; Tao, J.; Lu, X.; Zhu, Y.; Xia, Y. *Science* **2009,** *324,* 1302–1305.
(9) Wu, J.; Zhang, J.; Peng, Z.; Yang, S.; Wagner, F. T.; Yang, H. *J. Am. Chem. Soc.* **2010,** *132,* 4984–4985.
(10) Sun, S.; Murray, C. B.; Weller, D.; Folks, L.; Moser, A. *Science* **2000,** *287,* 1989–1992.
(11) Ge, J.; Hu, Y.; Yin, Y. *Angew. Chem., Int. Ed.* **2007,** *46,* 7428–7431.
(12) Na, H. B.; Lee, J. H.; An, K.; Park, Y.; Park, M.; Lee, I. S.; Nam, D.; Kim, S. T.; Kim, S.; Kim, S.; Lim, K.; Kim, K.; Kim, S.; Hyeon, T. *Angew. Chem., Int. Ed.* **2007,** *46,* 5397–5401.
(13) Dong, A. G.; Chen, J.; Patrick, M. V.; Kikkawa, J. M.; Murray, C. B. *Nature* **2010,** *466,* 474–477.
(14) Smith, A. M.; Nie, S. *Nat. Biotechnol.* **2009,** *27,* 732–733.
(15) Rosi, N. L.; Mirkin, C. A. *Chem. Rev.* **2005,** *105,* 1547–1562.
(16) Wu, S.; Han, G.; Milliron, D. J.; Aloni, S.; Altoe, V.; Talapin, D. V.; Cohen, B. E.; Schuck, P. J. *Proc. Natl. Acad. Sci. U.S.A.* **2009,** *106,* 10917–10921.
(17) Brust, M.; Walker, M.; Bethell, D.; Schiffrin, D. J.; Whyman, R. *J. Chem. Soc., Chem. Commun.* **1994,** 801–802.
(18) Xia, Y.; Xiong, Y. J.; Lim, B.; Skrabalak, S. E. *Angew. Chem., Int. Ed.* **2009,** *48,* 60–103.
(19) Murray, C. B.; Norris, D. J.; Bawendi, M. G. *J. Am. Chem. Soc.* **1993,** *115,* 8706–8715.
(20) Chen, O.; Chen, X.; Yang, Y.; Lynch, J.; Wu, H.; Zhuang, J.; Cao, Y. C. *Angew. Chem., Int. Ed.* **2008,** *47,* 8638–8641.
(21) Yu, W. W.; Falkner, J. C.; Shih, B. S.; Colvin, V. L. *Chem. Mater.* **2004,** *16,* 3318–3322.
(22) Park, J.; An, K.; Hwang, Y.; Park, J.; Noh, H.; Kim, J.; Park, J.; Hwang, N.; Hyeon, T. *Nat. Mater.* **2004,** *3,* 891–895.
(23) Shevchenko, E. V.; Talapin, D. V.; Rogach, A. L.; Kornowski, A.; Haase, M.; Weller, H. *J. Am. Chem. Soc.* **2002,** *124,* 11480–11485.
(24) Ye, X.; Collins, J. E.; Kang, Y.; Chen, J.; Chen, D. T. N.; Yodh, A. G.; Murray, C. B. *Proc. Natl. Acad. Sci. U.S.A.* **2010,** in press.

(25) Park, J.; Joo, J.; Kwon, S. G.; Jang, Y.; Hyeon, T. *Angew. Chem., Int. Ed.* **2007,** *46,* 4630–4660.
(26) Talapin, D. V.; Lee, J.-S.; Kovalenko, M. V.; Shevchenko, E. V. *Chem. Rev.* **2010,** *110,* 389–458.
(27) Law, M.; Luther, J. M.; Song, Q.; Hughes, B. K.; Perkins, C. L.; Nozik, A. J. *J. Am. Chem. Soc.* **2008,** *130,* 5974–5985.
(28) Kang, Y. J.; Murray, C. B. *J. Am. Chem. Soc.* **2010,** *132,* 7568–7569.
(29) Medintz, I. L.; Uyeda, H. T.; Goldman, E. R.; Mattoussi, H. *Nat. Mater.* **2005,** *4,* 435–446.
(30) Bruchez, M., Jr.; Moronne, M.; Gin, P.; Weiss, S.; Alivisatos, A. P. *Science* **1998,** *281,* 2013–2016.
(31) Chan, W. C. W.; Nie, S. *Science* **1998,** *281,* 2016–2018.
(32) Yu, D.; Wang, C.; Guyot-Sionnest, P. *Science* **2003,** *300,* 1277–1280.
(33) Zhang, T.; Ge, J.; Hu, Y.; Yin, Y. *Nano Lett.* **2007,** *7,* 3203–3207.
(34) Wu, H.; Zhu, H.; Zhuang, J.; Yang, S.; Liu, C.; Cao, Y. C. *Angew. Chem., Int. Ed.* **2008,** *47,* 3730–3734.
(35) Prakash, A.; Zhu, H. G.; Jones, C. J.; Benoit, D. N.; Ellsworth, A. Z.; Bryant, E. L.; Colvin, V. L. *ACS Nano* **2009,** *3,* 2139–2146.
(36) Wang, Y.; Wong, J. F.; Teng, X.; Lin, X. Z.; Yang, H. *Nano Lett.* **2003,** *3,* 1555–1559.
(37) Xie, J.; Xu, C.; Kohler, N.; Hou, Y.; Sun, S. *Adv. Mater.* **2007,** *19,* 3163–3166.
(38) Salgueirino-Maceira, V.; Liz-Marzán, L. M.; Farle, M. *Langmuir* **2004,** *20,* 6946–6950.
(39) Hong, R.; Fischer, N. O.; Emrick, T.; Rotello, V. M. *Chem. Mater.* **2005,** *17,* 4617–4621.
(40) Kim, S. B.; Cai, C.; Kim, J.; Sun, S.; Sweigart, D. A. *Organometallics* **2009,** *28,* 5341–5348.
(41) Wei, Y.; Yang, J.; Ying, J. Y. *Chem. Commun.* **2010,** *46,* 3179–3181.
(42) Kim, M.; Chen, Y.; Liu, Y.; Peng, X. *Angew. Chem., Int. Ed.* **2005,** *17,* 1429–1432.
(43) Kovalenko, M. V.; Scheele, M.; Talapin, D. V. *Science* **2009,** *324,* 1417–1420.
(44) Kovalenko, M. V.; Spokoyny, B.; Lee, J.-S.; Scheele, M.; Weber, A.; Perera, S.; Landry, D.; Talapin, D. V. *J. Am. Chem. Soc.* **2010,** *132,* 6686–6695.
(45) Tangirala, R.; Baker, J. L.; Alivisatos, A. P.; Milliron, D. J. *Angew. Chem., Int. Ed.* **2010,** *49,* 2878–2882.
(46) Huo, Z.; Tsung, C.-K.; Huang, W.; Fardy, M.; Yan, R.; Zhang, X.; Li, Y.; Yang, P. *Nano Lett.* **2009,** *9,* 1260–1264.
(47) Malakooti, R.; Cademartiri, L.; Akçakir, Y.; Petrov, S.; Migliori, A.; Ozin, G. A. *Adv. Mater.* **2006,** *18,* 2189–2194.
(48) Garcia-Otero, J.; Porto, M.; Rivas, J.; Bunde, A. *Phys. Rev. Lett.* **2000,** *84,* 167–170.
(49) Murray, C. B.; Sun, S.; Doyle, H.; Betley, T. *MRS Bull.* **2001,** *26,* 985–991.
(50) Kechrakos, D.; Trohidou, K. N. *Appl. Phys. Lett.* **2002,** *81,* 4574–4577.
(51) Bae, C. J.; Angappane, S.; Park, J. -G.; Lee, Y.; Lee, J.; An, K.; Hyeon, T. *Appl. Phys. Lett.* **2007,** *91,* 102502.
(52) Morup, S.; Tronc, E. *Phys. Rev. Lett.* **1994,** *72,* 3278–3281.
(53) Lutz, H. D.; Himmrich, J.; Schmidt, M. *J. Alloys Compd.* **1996,** *241,* 1–9.
(54) Gerlach, T.; Schütze, F.-W.; Baerns, M. *J. Catal.* **1999,** *185,* 131–137.
(55) Chen, W.; Kim, J.; Sun, S.; Chen, S. *J. Phys. Chem. C* **2008,** *112,* 3891–3898.
(56) Stamenkovic, V. R.; Mun, B. S.; Arenz, M.; Mayrhofer, K. J. J.; Lucas, C. A.; Wang, G. F.; Ross, P. N.; Markovic, N. M. *Nat. Mater.* **2007,** *6,* 241–247.
(57) Wang, C.; van der Vilet, D.; Chang, K.-C.; You, H.; Strmcnik, D.; Schlueter, J. A.; Markovic, N. M.; Stamenkovic, V. R. *J. Phys. Chem. C* **2009,** *113,* 19365–19368.
(58) Kim, J.; Lee, Y.; Sun, S. *J. Am. Chem. Soc.* **2010,** *132,* 4996–4997.